IEEE Control Systems Letters paper presented at
2023 62nd IEEE Conference on Decision and Control (CDC)
December 13-15, 2023. Marina Bay Sands, Singapore

Biomolecular Control Circuit with Inherent Bi-stability is Applicable for Automatic Detection of Gut Infection

Yulin Huang[1], *Graduate Student Member, IEEE*, and Michaëlle N. Mayalu[1], *Member, IEEE*

***Abstract*— Previously a variety of engineered biological circuits to control cell population have been developed. One possible implementation uses paradoxical feedback, where population control is achieved by using the same quorum sensing signal, produced and sensed by the cell population, to provide both positive (cell proliferation) and negative (cell death) feedback. Here, we extend the paradoxical feedback population control circuit with the addition of a detector to manipulate the activation of the circuit via modulation of an external signal. The detector design utilizes the inherent bi-stability within paradoxical feedback control to switch the cell population dynamics between two equilibrium states via an external signal. Through simulation, we first demonstrate that the bi-stability of the paradoxical feedback controller remains unaffected after the introduction of the detector. Also, the modified detector-population controller can automatically detect and respond to the external signal. We then show how the modified circuit can trigger the total elimination of the cell population using an additional external signal. Finally, we propose a solution for disturbance rejection by adjusting the concentration of a certain gene. Although the detector-population controller is used in the context of gut infection detection, it follows generalizable principles that can be used in various contexts.**

I. Introduction

A number of control theoretic tools from mechanical and electrical engineering have been adapted for the study and design of biological systems. These theoretic tools, with proper adjustments to fit the biological contexts, have been demonstrated efficiently for tackling problems in a variety of fields, from environment, to energy, to medicine. Researchers have demonstrated the ability and efficiency of feedback control of cell population both theoretically and experimentally [1], [2], [3]. Genetically engineered cell circuits made to implement negative feedback population control are shown to be capable of achieving robust perfect adaption for homeostasis [1]. However, the inherent design of the biomolecular circuits that implement negative feedback population control can lead to selection of mutated cells with aberrant proliferation leading to the failure of the controller.

To tackle this problem, the idea of paradoxical feedback controllers relying on quorum sensing signaling is proposed for the elimination of mutants and proper function of control. Quorum sensing is a process of bacterial cell-to-cell communication within one or between several populations [4]. An advantage of quorum sensing is the regulation of gene expression in response to fluctuations in cell-population density. Quorum sensing bacteria produce and release chemical signals that increase in concentration as a function of cell density. Genetically engineered cell circuits made to implement paradoxical feedback control have been shown to exhibit robustness against mutants experimentally (using mammalian cells) and theoretically (using bacterial cells) [2], [3]. The ability of paradoxical controllers to be robust against mutations is a useful feature for many applications including engineered cell therapies.

However, a missing feature in previous implementations of feedback population control is the ability to actively toggle (or switch) the cell population between multiple equilibrium points for further versatility of the design. In this paper, we develop a theoretical design of a detector that responds to external signals and examine its functionality in cooperation with a paradoxical feedback controller in bacteria. In biomolecular circuits, molecular species are subject to stochastic fluctuations, which could negatively impact the controller's performance on regulating downstream process [5]. The ideal design of the proposed detector-population controller will reject the disturbances due to the stochastic fluctuations in biomolecular circuits to prevent undesired operations of the controller. The intended application of the proposed design is for the development of a "living probiotic" bacterial system that can detect (and eventually treat) infection within the gut [6]. However, the design uses generalizable principles that are relevant for various contexts where external factors can trigger changes in a paradoxical feedback signal leading to biphasic responses in system behavior, such as in T-cell cell, Beta cell and nerve cell regulation [7].

II. Approach and Implementation

It is desired that the proposed detector can distinguish between combinations of distinct chemicals and make computations to manipulate the control circuit. In mechatronic terms, the detector resembles a relay in an electrical circuit which toggles the activation of the main circuit (see Figure 1a). With a proper genetic design of the detector, the population controller can be activated (i.e. switch from a low to high population equilibrium) automatically upon the detection of the external signal from the pathogen. Furthermore, the population controller can be turned off (i.e. population reduced to zero) upon detection of another orthogonal external signal. The performance and effectiveness of the controller should remain unaffected after the introduction of the detector.

*This work was supported by the Burroughs Wellcome Fund (PDEP Transition to Faculty Award).

[1] The authors are with the Department of Mechanical Engineering, Stanford University, Stanford, CA 94305 USA (e-mail: yuh245@stanford.edu; mmayalu@stanford.edu).

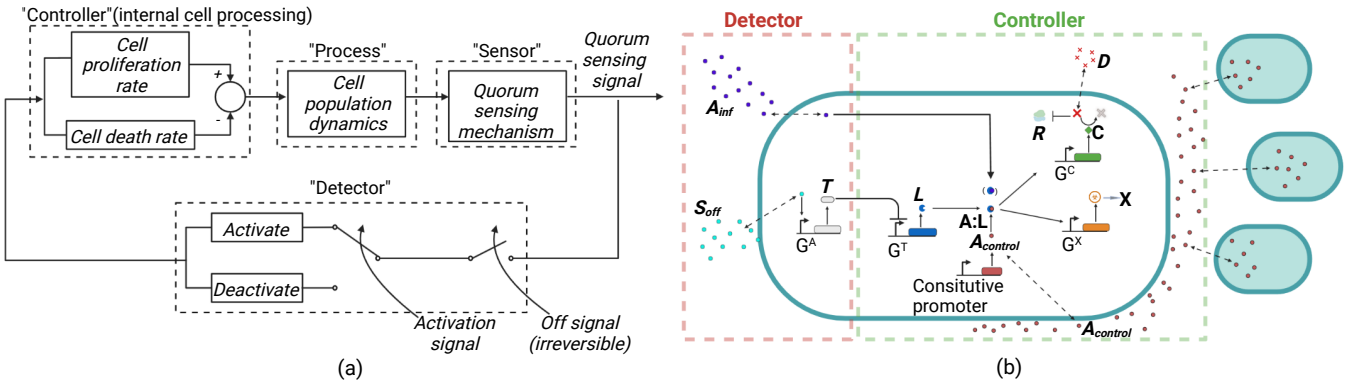

Fig. 1. (a) A block diagram shows how the detector-population controller uses a single quorum sensing signal to manipulate proliferation rate (positive feedback) and death rate (negative feedback) and drive the closed loop system dynamics. The detector serves as a switch to toggle or permanently shut down the controller upon detection of two distinct signals. (b) Schematic of the detector-population controller biomolecular design. The detector will activate the controller in the presence of pathogen signal (A_{inf}) when the total concentration of AHL ($A_{tot} = A_{control} + A_{inf}$) is above the activation threshold. The paradoxical controller consists of the AHL quorum sensing system (Quorum sensing signal, A , and its receiver, L), which forms a complex ($A:L$) to bind to and activate drug resistance gene, G^C (producing drug resistance protein, C), and cell death gene, G^X (producing cell lysis protein, X). The detector will shut down the controller when the "off" signal (S_{off}) is introduced. S_{off} activates a transcription repressor gene, G^A (producing transcription repressor , T). The transcription repressor binds to and inhibits AHL-receiver gene, G^T (inhibiting the production of AHL-receiver, L). As a result, the complex $A:L$ cannot be formed which will inhibit the downstream expression of the drug resistance. Without resistance, the drugs within the environment, D, will cause the cells to die out completely by binding to ribosomes, R, and inhibiting cell function. Figure adapted from [2].

Bi-stability is an inherent functionality in many biological systems [7]. It has been shown that the paradoxical feedback circuit can also exhibit bi-stability within the dynamics of population growth [2]. Here, we propose to design a biomolecular circuit that exploits the bi-stability property in order to activate the paradoxical controller upon the detection of a pathogen signal. The design is generalizable and can be adapted for other applications with careful choice of feedback signal and signal receptors [7]. For proof of concept, we modify the previously developed paradoxical feedback circuit in [2] which uses a single feedback signal to provide positive feedback (drug resistance induced cell proliferation) and negative feedback (toxin induced cell death) in different feedback signal concentration regimes.

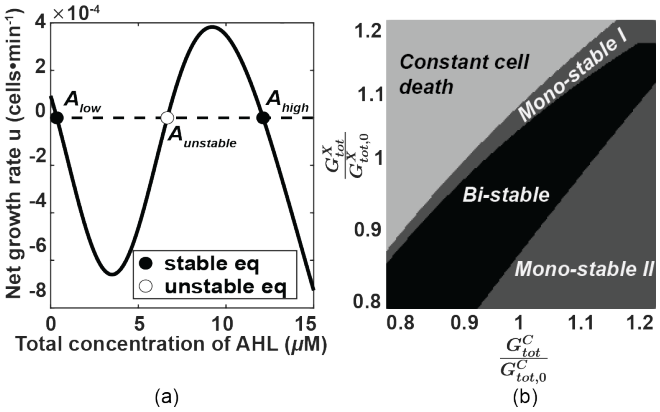

Fig. 2. (a) Net growth rate as a function of AHL for the engineered cells with paradoxical feedback control. Depending on the initial AHL concentration the final population will reach either the low or high stable equilibrium point. (b) Parameter sensitivity analysis reveals distinct stability regimes. The plot shows scaled concentration of G^C_{tot} vs G^X_{tot} from 0.8 to 1.2 of the originally chosen concentration ($G^C_{tot,0} = G^X_{tot,0} = 1\mu M$ [9]). There are four distinct regimes. Mono-stable type I (dark grey): only 2 eq. points, $A_{unstable}$ and A_{high} exist. Mono-stable type II (dark grey): only 2 eq. points, $A_{unstable}$ and A_{low} exist. Bi-stable (black): all three eq. points exist. Constant cell death (light grey): no eq. points exist.

For the pathogen, we consider *P. aeruginosa*, which can lead to gastrointestinal disorders, cystic fibrosis and gut-derived sepsis. *P. aeruginosa* is known to produce and secrete a specific small molecule *Acyl-homomserine lactone* (AHL) [6]. We therefore choose a homologous AHL as the feedback signal and a corresponding AHL-receiver protein (i.e. transcription factor) for the paradoxical feedback component within the biomolecular design of the detector-population controller [8].

As shown in Figure 1b, the control signal AHL, denoted $A_{control}$, will combine with its receiver, denoted L, to form a complex. The complex, denoted $A:L$, will adjust the functions of the positive and negative feedback in the downstream processes. More specifically, the $A:L$ complex will induce the production of a drug resistance protein, denoted C, that causes cell proliferation in the presence of drugs, denoted D, within the environment. The $A:L$ complex can also induce production of a toxin, denoted X, that causes cell death.

In the absence of the infection, the total concentration of AHL ($A_{tot} = A_{control}$) remains below the unstable equilibrium point (shown in Figure 2a) and the population size of the engineered cells remains low. When the infection occurs, the pathogen will produce a signal, denoted A_{inf}, and the signal can also combine with the AHL-receiver in the engineered cells. With a minimum threshold of pathogen signal, the controller will be activated when the total concentration of AHL ($A_{tot} = A_{control} + A_{inf}$) is above the unstable equilibrium point (shown in Figure 2a), expanding the population size of the engineered cells.

Besides the activation of the controller, we also propose to design a circuit component such that another external orthogonal "off" signal , denoted S_{off}, activates the production of a transcription repressor, denoted T, which subsequently

inhibits production of the AHL-receiver (L). As a result, the AHL/AHL-receiver complex ($A:L$) cannot be formed, which will inhibit the downstream expression of the drug resistance. Eventually, the engineered cells will die out due to the effects of the drugs present in the environment, leading to the complete shutdown of the controller.

We can then derive the dynamic equations of the detector-population controller from the reactions described in Figure1b. Equations (1) - (8) represent the dynamics of each species within the detector-population controller system.

$$\frac{dS_{off}}{dt} = \lambda_{S_{off}} - \delta_{S_{off}} \cdot S_{off} \tag{1}$$

$$\frac{dT}{dt} = k_{p,T} \cdot G^A_{tot} \cdot \frac{S^2_{off}}{K^2_T + S^2_{off}} - \delta_T \cdot T \tag{2}$$

$$\frac{dL}{dt} = k_{Lux} \cdot G^T - \delta_L \cdot L \tag{3}$$

$$\frac{dA_{control}}{dt} = N \cdot \nu_A - \delta_A \cdot A_{control} \tag{4}$$

$$\frac{dA_{inf}}{dt} = \lambda_{inf} - \delta_A \cdot A_{inf} \tag{5}$$

$$\frac{dC}{dt} = k_{prod,C} \cdot \frac{G^C_{tot} \cdot (A_{tot} - A_{gut})^2 \cdot L^2}{K_C + (A_{tot} - A_{gut})^2 \cdot L^2} - \delta_C \cdot C \tag{6}$$

$$\frac{dX}{dt} = k_{prod,X} \cdot \frac{G^X_{tot} \cdot (A_{tot} - A_{gut})^2 \cdot L^2}{K_X + (A_{tot} - A_{gut})^2 \cdot L^2} - \delta_X \cdot X \tag{7}$$

$$\frac{dN}{dt} = [(\psi_2 - \psi_1)\frac{R}{R+K} + \psi_1 - \delta_N X]N(1 - \frac{N}{N_{cap}}) \tag{8}$$

$$G^T = G^T_{tot} \frac{K^2_L}{K^2_L + T^2} \tag{9}$$

$$D = D_{tot} \frac{K_D}{K_D + C} \tag{10}$$

$$R = R_{tot} \frac{K_R}{K_R + D} \tag{11}$$

$$A_{tot} = A_{control} + \sigma \cdot A_{inf} \tag{12}$$

The following assumptions are applied for obtaining (1) - (8):

1) The production rates $k_{p,T}$ and k_{Lux} and degradation rates $\delta_{S_{off}}$, δ_T, and δ_L in (1) - (3) are constant.
2) Binding, dimerization, and enzymatic reaction dynamics are fast compared to the production and degradation of AHL, and hence they can be assumed to be at steady states.
3) The total concentrations of genes $G^T_{tot}, G^A_{tot}, G^C_{tot}, G^X_{tot}$ are conserved and set as constant parameters. The total concentrations of ribosomes R_{tot}, and drug D_{tot} are also conserved and set as constant parameters.

Equations (1) - (3) represent the dynamics for the off signal (S_{off}), the transcription repressor (T) and the AHL-receiver (L). In (1), $\lambda_{S_{off}}$ denotes the flux of the off signal. Equations (4) - (5) represent the dynamics for the control signal, $A_{control}$, and the infection signal, A_{inf}. In (5), ν_A denotes the production rate of $A_{control}$ and λ_{inf} represents the flux of infection signals from the pathogen. Once the infection occurs, λ_{inf} increases from zero and leads to production of A_{inf}, which is incorporated in the dynamics for the drug resistance protein, C, in (6) and the lysis protein, X, in (7).

Equation (8) describes the dynamics of the engineered cell population, N, which is considered homogeneous. Here, the net growth rate is a function of the amount of unbound ribosomes, R, and the lysis protein, X, within each cell. Parameters ψ_1 and ψ_2 are minimum death and maximum proliferation rates respectively. In equations (9) - (11) we have used simple binding kinetics to represent the following: 1) repression of the AHL-receiver gene, G^T, by the transcription repressor, 2) repression of the drug, D, by the drug resistance protein, 3) repression of unbound ribosomes by the drug.

There is a discounted binding strength when AHL-receiver, L, combines with the pathogen signal due to the slight difference between the homologous AHLs, $A_{control}$ and A_{inf} [8]. The discounted binding strength is taken into account by the parameter σ in (12). Furthermore, current studies have found evidence indicating AHL can be found in the human gut [10]. Taking this possibility into account, we incorporate the term A_{gut} in (6) and (7) to represent the amount of AHL natural to the human gut.

III. Theoretical Analysis

A. System Order Reduction

Using singular perturbation theory, we may re-write (1) - (8) in singular perturbation form [11]:

$$\begin{aligned} \tfrac{dx}{dt} &= f(x,y,\varepsilon) \\ \varepsilon \tfrac{dy}{dt} &= g(x,y,\varepsilon). \end{aligned} \tag{13}$$

Where:

$$\varepsilon = \frac{\delta_A}{\delta_X}, x = \begin{bmatrix} S_{off} \\ A_{control} \\ A_{inf} \\ N \end{bmatrix}, y = \begin{bmatrix} T \\ L \\ C \\ X \end{bmatrix}.$$

We define ε to be the ratio between the degradation rate of $A_{control}$ (δ_A) and the degradation rate of the toxin (δ_X). We assume the degradation rate of the toxin is on the same order as the drug resistance degradation, since these protein degradation rates can be adjusted with the use of degradation tags [2]. While this assumption holds, the AHL degradation is slow compared to the protein degradation, and ε can be set to zero.

The reduced slow system dynamics are given by:

$$\begin{aligned} \tfrac{dx}{dt} &= f(x,y) \\ g(x,y) &= 0. \end{aligned} \tag{14}$$

Where $f(x,y)$ is a 4×1 vector with elements equal to the right hand side of (1), (4), (5), (8) and $g(x,y)$ is a 4×1 vector with elements equal to the right hand side of (2), (3), (6), (7). Assuming reduced slow system dynamics and with the appropriate simplifications and substitutions, we may re-write the dynamics of the engineered cell population:

$$\frac{dN}{dt} = uN(1 - \frac{N}{N_{cap}}) \tag{15}$$

$$u = g(A_{tot}) - h(A_{tot}) \tag{16}$$

$$g(A_{tot}) = (\psi_2 - \psi_1)\frac{\bar{\mu_1}}{K_D}\frac{\bar{\mu_2} + (A_{tot} - A_{gut})^2 \cdot (G^T)^2}{\bar{\mu_3} + (A_{tot} - A_{gut})^2 \cdot (G^T)^2} + \psi_1 \tag{17}$$

$$h(A_{tot}) = \delta_N \frac{k_{prod,X}}{\delta_X}\frac{G^X_{tot} \cdot (A_{tot} - A_{gut})^2 \cdot (G^T)^2}{\bar{\gamma} + (A_{tot} - A_{gut})^2 \cdot (G^T)^2} \tag{18}$$

where $\bar{\mu_1}(\mu M)$, $\bar{\mu_2}(\mu M^2)$, $\bar{\mu_3}(\mu M^2)$,$\bar{\gamma}(\mu M^2)$ are lumped parameters that are a function of the binding rates, production rates, and dissociation constants described in Table I [2].

The reduced system can approximate the full system if the boundary layer system, which is defined by:

$$\frac{dy}{dt} = g(x, y) \tag{19}$$

is asymptotically stable [2]. Solving the eigenvalues of the linearized boundary layer system, we obtain the following:

$$e_1 = -\delta_T, e_2 = -\delta_L, e_3 = -\delta_C, e_4 = -\delta_X \tag{20}$$

These eigenvalues are all real and negative. Consequently, the reduced system can approximate the full system.

B. Existence of bi-stability

Since we rely on the bi-stability property of the detector-population controller system to activate the controller, it is necessary to determine the range of system parameters that guarantees the existence of bi-stability. Bi-stability is the direct result of the interplay between the positive and negative feedback loops within the system. Thus, we wish to observe how the change in strength of each feedback loop affects this property.

Examining (6) and (7), we notice that a strength change in either feedback loop is directly proportional to the changes in the total concentrations of the gene responsible for drug resistance induced proliferation, G^C_{tot} , and the gene responsible for toxin induced cell death, G^X_{tot}. These total gene concentrations are experimentally adjustable.

With this reasoning, we have determined the stability characteristics for a range of G^C_{tot} and G^X_{tot} concentrations to analyze the effects of positive and negative feedback on the bi-stability property of the system.

As can be seen in Figure 2b, there exists three regimes with distinct stability characteristics within the parameter space including the mono-stable (two types), bi-stable, and constant death regimes. Within the mono-stable type II regime, toxin production remains low allowing drug resistance induced cell proliferation to dominate at high concentrations of AHL. Within this regime, the high stable equilibrium point (A_{high}) does not exist, while the low stable (A_{low}) and middle unstable ($A_{unstable}$) points still remain. Within the bi-stable regime, toxin induced cell death and drug resistance induced cell proliferation are sufficiently balanced and all equilibrium points exist as shown in Figure 2a. Within the constant death regime, toxin production is too high and toxin-induced cell death dominates. No equilibrium points exist in this regime. Within the mono-stable type I regime, toxin production remains relatively high compared to drug resistance production but only strong enough to decrease the net growth rate such that the low stable (A_{low}) equilibrium point no longer exists while the unstable middle ($A_{unstable}$) and the high stable (A_{high}) points remain, which is contrary to the mono-stable type II regime.

To summarize, the control system will exhibit the desired bi-stability property with careful tuning of feedback strengths within a relevant parameter range. We may exploit this bi-stability property (which has been rigorously derived in [3]) for signal detection.

C. Range of Pathogen Signal Detection

It is necessary to determine the appropriate range that the detector will properly respond to the pathogen signal to activate the controller and expand the population of the engineered cells. Specifically, the total concentration of AHL (A_{tot}) in the system must be higher than the unstable equilibrium ($A_{unstable}$) and lower than the upper stable equilibrium (A_{high}) in order to have a positive net population growth rate (see Figure 2a):

$$A_{unstable} \leq A_{tot} \leq A_{high} \tag{21}$$

Substituting the steady state expression of $A_{control}$ and A_{inf} from (4) and (5), the following relationship is obtained:

$$\frac{A_{unstable} \cdot \delta_A - N \cdot \nu_A}{\sigma} \leq \lambda_{inf} \leq \frac{A_{high} \cdot \delta_A - N \cdot \nu_A}{\sigma} \tag{22}$$

As we can see from (22), the pathogen signal detection range depends on the equilibrium points of the system and the current population size. Therefore the sensitivity of the detector to the pathogen signal can be adjusted by shifting the equilibrium points of the system.

D. Disturbance Rejection

Another anticipated situation is the disturbance from stochastic fluctuations in the concentration of feedback signal, $A_{control}$. As described previously, pathogen signal A_{inf} will combine with the AHL-receiver as well to activate the controller when pathogen occurs. However, undesired fluctuations of $A_{control}$ might also turn on the controller even when there is no pathogen (i.e. when $\lambda_{inf} = 0$). Biomolecular concentration fluctuations are not rare, so the probability of accidentally turning the controller on due to the disturbance cannot be neglected [5].

Similar to the pathogen signal sensitivity, the disturbance rejection property of the system can also be modified by shifting the equilibrium points. However, increasing pathogen signal sensitivity will decrease disturbance rejection signifying a trade-off between these two system properties. Here, we will prioritize shifting the equilibrium points to optimize disturbance rejection.

We may derive an expression for the middle unstable ($A_{unstable}$) and high stable (A_{high}) equilibrium points as a

TABLE I

RANGE OF PARAMETER VALUES FOR SIMULATIONS.

Parameters	Description	Range
$k_{p,T}G^A_{tot}$, $k_{Lux}G^T$, $k_{prod,C}G^C_{tot}$, $k_{prod,X}G^X_{tot}$	Protein production	0.1 to 100 $(\mu M \cdot hr^{-1})$ [13]
δ_T, δ_L, δ_C, δ_X	Protein degradation rates	0.36 to 3.6 (hr^{-1}) [13]
K_R, K_D, K_T, K_L, K_C, K_X	Dissociation constants	10^{-7} to 10^6 (μM) [14]
δ_A , $\delta_{S_{off}}$	AHL and "off" signal degradation rate	~ 0.02 (min^{-1}) [15]

function of unbound AHL-receiver production gene, G^T:

$$A_{unstable} = \frac{6.30}{2G^T} + A_{gut} \tag{23}$$

$$A_{high} = \frac{17.23}{2G^T} + A_{gut} \tag{24}$$

where we have substituted biologically relevant values for all parameters in the above equations. As seen from (23) and (24), the equilibrium points of the system are inversely proportional to the concentration of G^T. When there is no external off signal (i.e. $S_{off} = 0$) and consequently no transcription repressor (i.e. $T = 0$), all AHL-receiver production genes are in their unbound state (i.e. $G^T = G^T_{tot}$), as verified by (9).

Because we only consider adjusting the disturbance rejection property in the absence of the off signal, we may vary the concentration of G^T_{tot} for this analysis. As discussed previously, the range of pathogen signal detection also depends on the equilibrium points of the system. This leads to a trade-off between detection sensitivity (early stage response to the gut infections) and disturbance rejection (robustness to fluctuations in feedback signal). The role of biological circuits that can buffer noise in both multiple stable states while maintaining the ability to switch between them is well known [12]. This principle suggests application of optimization for design specifications, which is a direction for future work.

IV. SIMULATION RESULTS

Simulations were performed to verify the design of the detector-population controller system. Table I describes system parameters and their biologically relevant ranges. Specifically, $K_T = K_L = 1\mu M$, $k_{p,T} = k_{Lux} = 1\mu M \cdot min^{-1}$, and $\delta_T = \delta_L = 1 min^{-1}$. Values for all other parameters were taken directly from [2]. Figure 3a shows the time evolution of the population of engineered cells under different initial conditions. As can be seen, the bi-stability property of the paradoxical controller is maintained for both the full and reduced order systems. The simulation results demonstrate that the introduction of the detector does not affect the original performance and properties of the paradoxical feedback controller. Therefore, the design of the detector with the chosen genetic components is adequate for automatic pathogen detection realized using the inherent bi-stability property within the paradoxical feedback circuit architecture. Figure 3c shows the ability of the detector to activate and

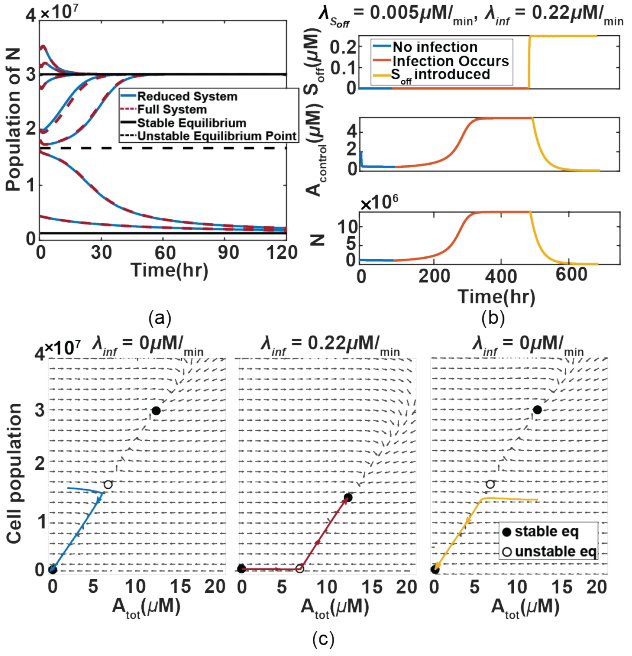

Fig. 3. (a) Simulation results for the reduced system (blue solid lines) and the full system (red dashed lines). Both systems posses the inherent bi-stability property for the paradoxical signaling controller. (b) Shut Down Process. The plots show that the controller is activated and remains on when the infection occurs (red regions of trajectories). The external signal (S_{off}, top plot) terminates the controller (yellow regions of trajectories) by reducing the population (N, bottom plot) to zero. The middle plot shows the dynamics of $A_{control}$ during the termination process. (c) Modified eq. points due to presence of pathogen signal. Left: Initial population size is below the unstable eq. point and converges to the low stable eq. point. Middle: The pathogen signal is introduced leading to population expansion above the unstable eq. point and final convergence at the high stable eq. point. However, the population does not reach the original high eq. point value due to the modification of system dynamics with the introduction of pathogen signal. Right: The population returns back to the eq. point when the infection is removed from the environment. The system eq. points revert back to their original positions after the removal of pathogen.

deactivate the paradoxical controller. If there is no infection, the term λ_{inf} in (5) is zero, and the detector will not activate the controller. Consequently, the population of the engineered cells will be driven to the low stable equilibrium point (blue trajectory of left plot in Figure 3c). On the other hand if the infection occurs, λ_{inf} is no longer zero which leads to the increase in the concentration of A_{inf} and, as a result, A_{tot}. The increase of A_{tot} initiates the activation of the controller and the subsequent increase in population of the engineered cells (red trajectory in middle plot of Figure 3c). After the controller is activated, the population of the engineered cells is maintained at the high stable equilibrium point. When the infection is removed from the environment, the population will shift back to the low stable equilibrium point (yellow trajectory in Figure 3c).

The introduction of the external pathogen signal changes the system dynamics leading to a relocation of the equilibrium points as seen in Figure 3c (middle plot). When the external signal is removed, the equilibrium points revert back to their original locations before the pathogen was introduced.

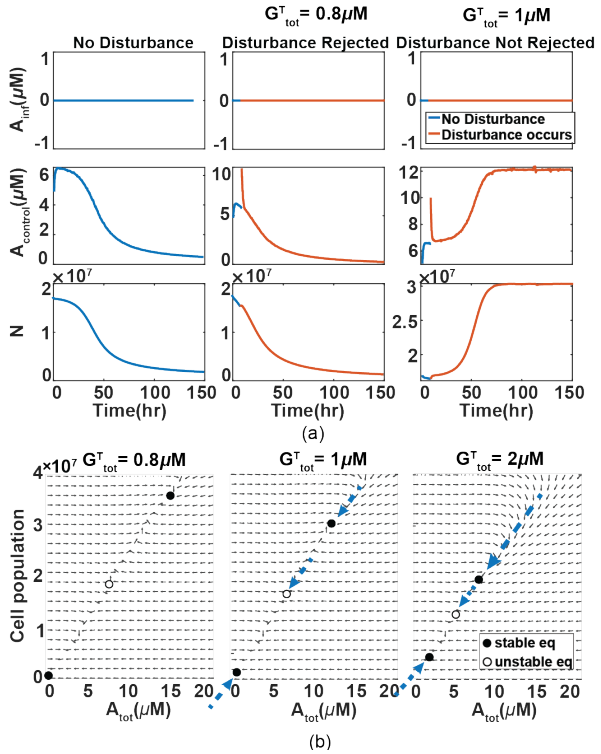

Fig. 4. (a) Stochastic fluctuation occurs inside the system. Left column: The controller remains off when there is no infection ($\lambda_{inf} = 0$). Right column: A fluctuation of the concentration of $A_{control}$ undesirably turns on the controller even when there is no infection. Middle column: Disturbance is rejected by lowering the concentration of G^T_{tot}. The same fluctuation no longer accidentally activates the controller. Simulations are performed with signal-to-noise ratio of 0.1dB [16]. (b) Phase diagrams of the detector-population controller system for three different concentrations of G^T_{tot}. The diagrams demonstrate that the sensitivity of the system decreases by decreasing the concentration of G^T_{tot}, and consequently leads to disturbance rejection.

Figure 3b shows how when the off signal (S_{off}) is introduced, it can completely shut down the controller. In this case, the term $\lambda_{S_{off}}$ in (1) is no longer zero and the population of the engineered cells is completely removed (reduced to zero) instead of going to the low stable equilibrium. This adds an extra mechanism of safety (or "kill switch") that can be used to completely remove all engineered cells from the gut.

The simulation results in Figure 3 verify the ability of the detector to activate, deactivate, and terminate the controller. However, as discussed previously, a fluctuation in the concentration of feedback signal, $A_{control}$, could lead to undesired activation of the controller (as shown in Figure 4a, right). In the previous section, we proposed the solution to reject disturbances by changing the total concentration of the AHL-receiver production gene, G^T_{tot}. As shown in Figure 4a (middle), by decreasing G^T_{tot}, the same fluctuation will no longer accidentally turn on the controller. In Figure 4b, we further verify how the equilibrium points of the system shift to higher values when the concentration of G^T_{tot} is decreased. The simulation results in Figure 4 verify the feasibility and effectiveness of our proposed solution to provide rejection to disturbances in the feedback signal.

V. CONCLUSIONS

In this paper, we propose and develop a detector design that serves as an activation mechanism for the paradoxical controller. The performance and properties of the detector-population controller system are verified with simulations. The bi-stability of the paradoxical controller is maintained within the detector-population controller system, and the detector successfully reacts to different signals to manipulate the paradoxical controller. We also propose and verify the feasibility of a solution to reduce effects of a specific disturbance inside the system to prevent undesired activation of the controller by lowering the total concentration of a gene, G^T_{tot}. The detector-population controller system provides a more sophisticated population control of genetically engineered circuits, grants more safety, and introduces automation within the design. Future work will involve experiments based on the selection of circuit components to validate the feasibility of the design and ensure all circuit components function properly.

REFERENCES

[1] M. H. Khammash, "Perfect adaptation in biology," *Cell Systems*, vol. 12, pp. 509–521, 6 2021.

[2] M. N. Mayalu and R. M. Murray, "Theoretical design of paradoxical signaling-based synthetic population control circuit in e. coli.", bioRχiv, 1 2020.

[3] Y. Ma, M. W. Budde, M. N. Mayalu, J. Zhu, A. C. Lu, R. M. Murray, and M. B. Elowitz, "Synthetic mammalian signaling circuits for robust cell population control," *Cell*, vol. 185, pp. 967–979.e12, 3 2022.

[4] M. M. Vasconcelos, U. Mitra, O. Camara, K. P. Silva, and J. Boedicker, "Bacterial Quorum Sensing as a Networked Decision System," in *2018 IEEE International Conference on Communications (ICC)*, pp. 1–6.

[5] V. Hsiao, A. Swaminathan, and R. M. Murray, "Control theory for synthetic biology: Recent advances in system characterization, control design, and controller implementation for synthetic biology," *IEEE Control Systems*, vol. 38, pp. 32–62, 6 2018.

[6] S. Gupta, E. E. Bram, and R. Weiss, "Genetically Programmable Pathogen Sense and Destroy," *ACS Synthetic Biology*, vol. 2, no. 12, pp. 715–723,6 2013.

[7] O. Karin and U. Alon, "Biphasic response as a mechanism against mutant takeover in tissue homeostasis circuits," *Molecular Systems Biology*, vol. 13, no. 6, p. 933, 6 2017.

[8] N. Kylilis, Z. A. Tuza, G.-B. Stan, and K. M. Polizzi, "Tools for engineering coordinated system behaviour in synthetic microbial consortia," *Nature Communications*, vol. 9, no. 1, p. 2677, 7 2018.

[9] D. I. Cattoni, O. Chara, S. B. Kaufman, and F. L. González Flecha, "Cooperativity in Binding Processes: New Insights from Phenomenological Modeling," *PLoS ONE*, vol. 10, no. 12, p. e0146043, 12 2015.

[10] G. Coquant, J. P. Grill, and P. Seksik, "Impact of n-acyl-homoserine lactones, quorum sensing molecules, on gut immunity," 8 2020.

[11] D. D. Vecchio, A. J. Dy, and Y. Qian, "Control theory meets synthetic biology," *Journal of the Royal Society Interface*, vol. 13, 7 2016.

[12] M. Chen, L. Wang, C. C. Liu, and Q. Nie, "Noise Attenuation in the ON and OFF States of Biological Switches," *ACS Synthetic Biology*, vol. 2, no. 10, pp. 587–593, 6 2013.

[13] X. Ren, C. C. Samaniego, R. M. Murray, and E. Franco, "Bistable State Switch Enables Ultrasensitive Feedback Control in Heterogeneous Microbial Populations," in *2021 American Control Conference (ACC)*, pp. 652–659.

[14] S. Erlendsson and K. Teilum, "Binding Revisited—Avidity in Cellular Function and Signaling," *Frontiers in Molecular Biosciences*, vol. 7, 1 2021.

[15] R. Milo, P. Jorgensen, U. Moran, G. Weber, and M. Springer, "BioNumbers–the database of key numbers in molecular and cell biology," vol. 38, pp. D750–753, 1 2010.

[16] J. Beal, "Signal-to-Noise Ratio Measures Efficacy of Biological Computing Devices and Circuits," *Frontiers in Bioengineering and Biotechnology*, vol. 3, 6 2015.